Advanced Powder Technology 32 (2021) 3161–3173

Contents lists available at ScienceDirect

Advanced Powder Technology

journal homepage: www.elsevier.com/locate/apt

Original Research Paper

Construction and characterization of a novel Tenofovir-loaded PEGylated niosome conjugated with TAT peptide for evaluation of its cytotoxicity and anti-HIV effects

Maryam-Sadat Yadavar-Nikravesh [a,b], Saeedeh Ahmadi [a], Alireza Milani [b], Iman Akbarzadeh [a,c], Mehdi Khoobi [d,e], Rouhollah Vahabpour [f], Azam Bolhassani [b,*], Haleh Bakhshandeh [a,*]

[a] Nanobiotechnology Department, New Technologies Research Group, Pasteur Institute of Iran, Tehran, Iran
[b] Department of Hepatitis, AIDS and Blood Borne Diseases, Pasteur Institute of Iran, Tehran. Iran
[c] Department of Chemical and Petrochemical Engineering, Sharif University of Technology, Tehran, Iran
[d] Department of Medicinal Chemistry, Faulty of Pharmacy, Tehran University of Medical Science, Tehran, Iran
[e] Biomaterials Group, Pharmaceutical Science Research Center, The Institute of Pharmaceutical Science (TIPS), Tehran University of Medical Science, Tehran, Iran
[f] Department of Medical Lab Technology, School of Allied Medical Sciences, Shahid Beheshti University of Medical Sciences, Tehran. Iran

ARTICLE INFO

Article history:
Received 7 January 2021
Received in revised form 1 April 2021
Accepted 25 May 2021
Available online 31 July 2021

Keywords:
Tenofovir
Niosome
TAT
PEGylation
Anti-Scr HIV

ABSTRACT

In recent years, nanocarriers have become potent drug delivery system candidates, especially in anti-HIV therapies. Meanwhile, using cell-penetrating peptides such as TAT for improvement of cellular transportation has been widely noticed. In the current study, a novel PEGylated niosomal formulation (PEG-NI) loaded with an anti-HIV drug (Tenofovir) has been prepared by using thin-film hydration method based on cholesterol and Span 60 surfactant. Then, the TAT peptide was incorporated into optimized PEGylated niosome. Further morphological and *in vitro* studies were performed by TAT conjugated (TAT-NI1) and PEGylated niosomes. The average size, polydispersity index and encapsulation efficiency of Tenofovir-loaded TAT-NI1 were 208 ± 9.004 nm, 0.39 ± 0.008 and 75 ± 2.516%, respectively. The cytotoxicity effects of TAT-NI1 and PEG-NI niosomes were analyzed by MTT assay in comparison with Tenofovir. The IC50 of PEG-NI, empty PEG-NI, TAT-NI1, free Tenofovir and TAT peptide were 65.41, 37.04, 41.02, 43.07, and 37.12, respectively. Furthermore, the inhibitory effects of samples against the HIV infected HeLa cells were evaluated. The results displayed a higher cytotoxicity, lower anti-Scr HIV effect and improved Tenofovir release profile for TAT-NI1 in comparison with PEG-NI. Overall, this study revealed that PEGylation is a superior alternative rather than TAT conjugation in anti-HIV drug delivery systems.

1. Introduction

The human immunodeficiency virus type 1 (HIV1) is a lentivirus and an example of genus retroviruses which targets the CD4 + lymphocytes. Theoretically, acquired immunodeficiency syndrome (AIDS) occurs when the blood CD4 count drops below 200 cells/μL [1,2]. The reports showed that in 2019 about 38 million individuals were infected by HIV in which is increased by 1.7 million people annually [3]. Early diagnosis and treatment of patients would prevent HIV transmission and increase their lifespan from 1 year to over 10 years, recently [4]. Various prevention and therapeutic strategies have been performed to stop the progression of HIV in all over the world [5]. HIV is localized and hidden in certain inaccessible compartments of the body, such as the CNS where it cannot be reached by the majority of therapeutic agents easily. Tenofovir is an HIV reverse transcriptase inhibitor, which is prescribed as first-line AIDS therapy. The low toxicity, long plasma half-life of about 17 h, and convenient dosing of 300 mg per day of Tenofovir made it favored in HIV/AIDS-burdened countries. Although Tenofovir has hydrophobic nature (log p: 1.25) but its penetration against the biological barriers is low (about 25%) [6,7].

Particles are used as an active or inactive pharmaceutical ingredient in drug formulation, so powder technology is occupied to design enhanced solid dosage forms based on the properties of their particles. Consequently, small sized like Nano or micro sized particles have prominent role in particle technology's perspective [8]. Nanoparticle-based drug delivery systems have led to efficacy improvement, toxicity reduction, sustained release provision and

* Corresponding authors.
E-mail addresses: A_bolhasani@pasteur.ac.ir (A. Bolhassani), h_bakhshandeh@pasteur.ac.ir (H. Bakhshandeh).

https://doi.org/10.1016/j.apt.2021.05.047

bioavailability enhancement of drugs to treat chronic human diseases. Niosomes are the nanocarrier systems based on the self-assembly of cholesterol and non-ionic surfactants. Niosomes are more stable and cheaper in contrast with liposomes that can deliver different types of drugs including synthetic or natural active ingredients which is due to the usage of non-ionic surfactants [9–14]. Niosomes are biodegradable and biocompatible, which can increase gastric absorption, improve shelf life, reduce the toxicity of drugs and also can be functionalized for targeted drug delivery. Targeted nanodrug delivery systems can deliver nanocarriers specifically via adsorption or surface ligand attachment to the targeted organs, thereby they can expand the therapeutic window, accumulate drug in the targeted organ and improve drug bioavailability [15,16]. PEGylation of nanocarriers can prevent carriers binding to plasma proteins and removal by RES, so they can prolong circulation time and accumulate nanocarriers in infected tissue via enhanced permeability and retention time (EPR effect). Also, by means of PEGylation on the surface of nanoparticles, the hydrophobicity can be changed, targeted delivery achieved and controlled drug release will be generated. Moreover, PEGylated nanocarriers can be easily functionalized to conjugate various targeting moieties for the efficient delivery of drugs to the target cell [17–19]. DSPE-PEG-Maleimide is a commercially available PEGylated lipid that has been widely used for preparation of targeted lipid-based drug delivery systems such as niosomes which is due to its coupling efficiency and stable covalent bond with ligands containing thiol group like antibodies and cell-penetrating peptides (CPPs) [20–22].

Cell-penetrating peptides, as a class of short peptides with cell membrane translocation properties, are widely used for delivery of various types of cargoes such as small molecules, proteins, MABs and nucleic acids across the biological membrane especially blood-brain barrier efficiency (BBB) [23]. This process of traversing the cell membrane is termed protein transduction and is usually confined to a domain of <20 amino acids, designated as the protein-transduction domain (PTD) [24]. One example of well-known CPP is cationic TAT peptide (AYGRKKRRQRRR) which is the basic region of the *trans*-activating transcriptional activator protein from HIV-1 and it is essential for viral replication. Furthermore, this peptide is well-known due to its non-immunogenicity and low cytotoxicity properties [25]. Also, this CPP can improve different nanocarriers transportation across biological barriers via energy independent pathway, such as the blood-brain barrier so it can be taken up by brain infected cells [26,27].

Design of experiment (DOE) is a statistically tool which provides a study for investigation of most critical promoters and their impact on formulation of nanoparticle with ideal attribute via at least experiment and cost. One example of DOE study is Response surface methodology (RSM) which can effectively optimized nanoparticle formulation process. In this regard, the relationship of multifactor on response variables is considered [28–32]. The study aimed to investigate the inhibitory effect of TAT peptide conjugated niosome on Scr HIV replication for the first time. Optimized PEGylated noisome which was loaded with Tenofovir, prepared based on the optimum molar ratio of Span 60 to cholesterol and drug to lipid and then functionalized by TAT cell-penetrating peptide. Optimum condition obtained by Response surface methodology (RSM). Accordingly, physicochemical properties such as mean size, PDI and encapsulation efficacy were analyzed. The *in vitro* drug release profile, cytotoxicity, and anti-Scr HIV activity of empty PEGylated niosome (empty PEG-NI), Tenofovir-loaded PEGylated niosome (PEG-NI) and Tenofovir-loaded TAT conjugated niosome (TAT-NI1) was studied. Cellular uptake of optimum Tenofovir-loaded TAT conjugated noisome was evaluated by confocal electron microscopy.

2. Materials and methods

2.1. Chemicals

Tenofovir was received as a gift from Bakhtar Bioshimi Co. Sorbitan monostearate (Span 60), Cholesterol, Chloroform, Methanol, Phosphate buffer solution (PBS), 1,2-distearoyl-*sn*-*glycero*-3-phosphoethanolamine-N-[methoxy(polyethylene glycol)-2000] (mPEG2000-DSPE) were purchased from Lipoid (Ludwigshafen, Germany). 1, 2-distearoyl-*sn*-*glycero*-3-phosphoethanolamine-N-[maleimide (polyethylene glycol)-2000] (ammonium salt) (Mal-PEG2000-DSPE) was obtained from Avanti Polar Lipids (Alabaster, AL), Cys-TAT peptide was received from bio basic. Iodine powder, TLC silica gel and Amicon filter (Ultra-15-Membrane, MWCO 3000 and 30000 Da) were bought from Sigma Aldrich (St. Louis, Missouri, United States). Dialysis membrane (MWCO 12000 Da) and MTT (Methyl thiazolyl diphenyl-tetrazolium bromide) were obtained from Sigma Aldrich (USA). Medium RPMI-1640, DMEM (Dulbecco's Modified Eagle Medium) and Penicillin/Streptomycin (PS) were purchased from Gibco, (USA). P24 assay kit was obtained from Abcam, USA. Deionized water was used as an aqueous medium.

2.2. Synthesis of TAT conjugated DSPE-PEG

DSPE-PEG2000-Maleimide was reacted with Cys-TAT peptide (1:1.5 M ratio) in chloroform/methanol (2:1 v/v) under Argon atmosphere at room temperature and stirring condition for 48 h. The coupling reaction was traced by thin-layer chromatography with a mobile phase of chloroform/methanol/deionized water/NH3 (83: 12: 2.3: 2.3 v/v) as well as iodine vapor exposure afterward. After the disappearance of the DSPE-PEG-Mal spot on the TLC, the organic solvent was evaporated by a rotary evaporation procedure. For removing a trace amount of excess Cys-TAT, the resulting thin film was hydrated in PBS (pH 7.4) and filtrated with Amicon ultrafilter (MWCO 3000 Da). Then the supernatant was evaporated under vacuum condition, freeze-dried and stored at −20 °C until noisome preparation step. Formation of the conjugate was confirmed by H NMR and FTIR [33–37].

2.3. Design of the experiments and formulation optimization using RSM

Response surface methodology is widely used in order to investigate the effective preparation parameters in the optimization of nanoparticles. Accordingly, two-factors (molar ratios of Span 60/Cholesterol and Lipid/Drug) and their levels were represented in Table 1. These levels were defined by literature review and screening study [34–48]. The effect of these variables was examined on the mean size (nm), polydispersity index (PDI) and entrapment efficiency (EE). The optimum formulation was selected based on the minimum size and polydispersity index range of the niosomes and the maximum range of entrapment efficiency.Table 2.

Table 1
RSM experimental parameters and levels for preparation of nanoparticles.

Independent variable	levels		
	Low	Medium	High
X_1 = Molar ratio of lipid/drug	10	15	20
X2 = Molar ratio of Span 60/Cholesterol	0.5	1	2
Dependent variable	**Constraints**		
Y1 = Particle size	Minimum		
Y2 = PDI	Minimum		
Y4 = EE	Maximum		

Table 2
Design of experiments using response surface methodology (RSM) to optimize the niosomal formulation of Tenofovir.

Sample ID	lipid/drug (Molar ratio)	Span 60/Cholesterol (Molar ratio)	Molar composition[1] (%)
PEG-NI1	0.5	2	9.1:28.8:57.6:4.5
PEG-NI 2	0.5	1	9.1:43.2:43.2:4.5
PEG-NI 3	0.5	0.5	9.1:57.6:28.8:4.5
PEG-NI 4	2	2	4.7:30.3:60.5:4.5
PEG-NI 5	2	1	4.7:45.4:45.4:4.5
PEG-NI 6	2	0.5	4.7:60.5:30.3:4.5
PEG-NI 7	1	2	6.2:29.8:59.6:4.5
PEG-NI 8	1	1	6.2:44.6:44.6:4.5
PEG-NI 9	1	0.5	6.2: 29.8:59.6:4.5

1: Molar composition of Tenofovir: Cholesterol: Span 60: DSPE-PEG-PE in percent.

Design-Expert® V10.0.1 software (Stat-Ease, Inc., Minneapolis, MN, USA) was used for the experimental designs and the regression analysis of the experimental data. The significance of the data was evaluated using ANOVA. Many perturbations and three-dimensional (3D) surface plots were drawn to illustrate the effects of the factors on the responses. The significance and the importance of the variable's effects and their interactions were determined by using probability value (p value). The fitness of the model was checked by the coefficient of determination (R^2) and signal to noise (F-test) for ANOVA [49].

2.4. Preparation of Tenofovir-loaded niosomes

Nanoparticles were prepared by thin-film hydration method using rotary evaporator. The synthesized niosomes included in this study were PEGylated niosome (PEG-NI) and TAT conjugated niosome (TAT-NI) which were loaded with Tenofovir. In order to achieve the optimized formulation of Tenofovir-loaded PEGylated niosome, different amounts of Span 60, cholesterol and Tenofovir, which were obtained by RSM, (the molar ratio of lipid/drug were 10, 15, 20 and span 60/cholesterol were 0.5, 1 and 2) and constant molar percent of DSPE-PEG-PE (4.5%), were dissolved in an organic solvent (chloroform, 10 ml), followed by evaporation of chloroform using a rotary evaporator (120 rpm, 60 °C, 30 min). Then, the dried thin films were hydrated using the PBS (pH7.4) at 37 °C for 60 min. Finally, the samples were sonicated for 3 min via probe sonicator in ice bath to obtain niosomes with uniform size distribution.

The ingredient molar composition of optimized PEG-NI is represented in Table 3 (the molar percent of Tenofovir, Cholesterol, Span 60 and DSPE-PEG-PE were9.1, 45.6, 41.1 and 4.2percent respectively). This formula was used for the TAT-NI niosomes formulation. Accordingly, 3 different molar compositions of DSPE-PEG-TAT, DSPE-PEG-PE, Span 60, Cholesterol, and Tenofovir were used for TAT-NI niosomes preparation (Table 4) [24]. After physical characteristics investigation of TAT-NI niosomes (encapsulation efficiency, mean particle size, Poly disperse index and zeta potential), the best one (TAT-NI1; the molar percent of Tenofovir, Cholesterol, Span 60, DSPE-PEG-PE and DSPE-PEG-TAT was 9.1:45.6:41.1:2.3:2.3) were lyophilized with a cryo-protectant and stored at −20 °C for further characterization studies.

Table 3
Different molar composition of optimized Tenofovir-loaded PEGylated niosome.

Sample ID	lipid/drug (Molar ratio)	Span 60/Cholesterol (Molar ratio)	Molar composition[1] (%)
PEG-NI	10	0.9	9.1:45.6:41.1: 4.2

1: Molar composition of Tenofovir: Cholesterol: Span 60: DSPE-PEG-PE in percent.

2.5. Characterization of Tenofovir-loaded niosomes

2.5.1. Encapsulation efficiency (EE)

The encapsulation efficiency (EE) of formulations was evaluated by the ultrafiltration method. The solution containing drugs loaded niosomes was ultra-filtered at 4000×g for 20 min using an Amicon Ultra filter (MWCO 30,000 Da). During filtration, the Tenofovir containing niosomes remained in the top chamber and free drugs moved through the filter membrane. The concentration of each drug was measured by UV visible spectroscopy (JASCO V-530, Japan) at a wavelength of 270 nm. The entrapment efficiency percent was calculated by using the following equation.

$$\text{EncapsulationEfficiency}(\%) = [(A - B)/A] * 100 \quad (1)$$

Where A is the amount of initial drug entrapped into the niosomal formulations and B is the amount of free drug passed through the membrane.

2.5.2. Size distribution and polydispersity index

Mean size and polydispersity index (PDI) of freshly hydrated niosomes were examined by Zetasizer Nano ZS at 25 °C, using a 45 mm focus lens and a beam length of 2.4 mm (Malvern Instrument ltd. Malvern, UK). Zeta potential was measured to evaluate the surface charge on the functionalized and optimized niosomes and functionalized niosome stability [50]. 1 ml of the sample was tested in a polystyrene cuvette. Three independent measurements were conducted and the results were reported as mean ± SD (see supplementary information, Fig. S1).

2.5.3. Morphological study

The morphology of the best sample was determined by scanning electron microscopy (SEM). In this regard, 500 μl of lyophilized Tenofovir-loaded TAT-NI1 were diluted in 2 cc deionized water and then 5 μl of the sample was loaded on a glass slide and dried overnight. The sample was coated with gold particles of 100 Å for 3 min under Argon atmosphere using a sputter in a high vacuum evaporator. Then it was visualized in a FE-SEM (voltage of 15 kV and current of 0.5 mA; FEI Nova NanoSEM 450 Bruker X Flash 61 10) To notice the size and shape of the nanoparticles.

2.5.4. Fourier transform infrared spectroscopy (FTIR)

FTIR analysis was performed to confirm the conjugation of peptide to lipid and drug-carrier interaction. So FTIR spectra of pure Tenofovir disoproxil fumarate (TDF), Span 60, Cholesterol, Tenofovir-loaded TAT-NI1 and empty TAT-NI1 were recorded and scanned in the region between 4000 cm^{-1} and 400 cm^{-1} and res-

Table 4
Different molar composition of TAT of functionalized noisome.

Sample ID	lipid/drug(Molar ratio)	Span 60/Cholesterol (Molar ratio)	DSPE-PEG-PE/DSPE-PEG-TAT(Molar ratio)	Molar composition[1] (%)
TAT-NI1	10	0.9	1	9.1:45.6:41.1:2.3:2.3
TAT-NI2	10	0.9	0.5	9.1: 45.6:41.1:5:3
TAT-NI3	10	0.9	2	9.1: 45.6:41.1:3:1.5

1: Molar composition of Tenofovir: Cholesterol: Span60: DSPE-PEG-PE: DSPE-PEG-TAT in percent.

olution of 0.5 cm^{-1} by using Perkin Elmer Spectrum FTIR spectrophotometer version 10.03.06, USA.

2.5.5. Differential scanning calorimetry (DSC)

Empty and Tenofovir-loaded TAT-NI1 were dried before DSC analysis by using a freeze drier. 5 mg of each sample were sealed in an aluminum pan and then analyzed under nitrogen atmosphere with a heating range from 30 °C to 300 °C with a scanning rate of 10 °C/min. The baseline was recorded with a blank aluminum pan as a Ref. [51].

2.5.6. Confocal electron microscopy

Cellular uptake of TAT conjugated model drug-loaded niosome was evaluated with confocal laser scanning microscopy. Accordingly, 10^5 HeLa cells/mL were seeded in DMEM medium with FBS 10%, on 20 × 20 mm coverslips overnight. Then HeLa cells were treated with 1 ml Nile red loaded TAT-NI1 which was diluted with 1 ml DMEM medium and incubated at 37 °C for 16 h. the cells were washed three times with 1 ml PBS 10% and fixed with 4% paraformaldehyde (PFA) for 4 min at room temperature. Then the HeLa cells were stained with coumarin-6 to stain plasma membrane and imaged by a laser scanning confocal electron microscope. [52]

2.5.7. In vitro drug release

Sustained drug release is an important property of nanoscale drug delivery systems that will minimize the side effects of the drug [53]. For evaluation of the drug release pattern of PEG-NI, TAT-NI1 and free Tenofovir, the dialysis method was used [54]. Accordingly, free drug, the lyophilized PEG-NI and TAT-NI1 were dispersed in 1.5 ml PBS (pH 7.4), and then were dialyzed against 15 ml PBS (pH 7.4) for a total period of 72 h at 37 °C on a magnetic stirrer. The released drug in 1 ml aliquots at specific intervals (0.5, 1, 2, 4, 6, 24, 48 and 72 h) was analyzed by UV spectrophotometer at a wavelength of 270 nm [54,55]. The calibration curve was plotted over concentration range of 10–100 μg/ml (supplementary information, Fig.S2.) and the proposed method was validated for precision, accuracy, linearity, limit of detection (LOD) and limit of quantitation (LOQ) (supplementary information, Table S1).

2.5.8. MTT assay

3-(4, 5-Dimethylthiazol-2-yl)-2, 5-diphenyl tetrazolium bromide (MTT) assay were used to determine the cytotoxicity of the niosomal formulations. Hela cells (10^4 cells/well) were seeded in 96-well plate in a volume of 100 μl and cultivated for 24 h at 37 °C. After replacement with fresh medium (DMEM medium with FBS 10%), cells were treated with the pure drug, drug-loaded PEG-NI, TAT-NI1, Empty PEG-NI and free TAT peptide at different concentrations (Table 8) for 48 h. Then, 200 μl of 0.05 mg/ml MTT solution was added and incubated for 4 h at 37 °C. The media were removed and replaced with isopropanol and incubated for 15 min at 37 °C. Finally, UV adsorptions were analyzed by UV ELISA reader at 570 nm wavelength [56]. The effects of cell cytotoxicity were determined by Eq. (2).

$$\frac{ODtest - ODcontrol}{ODcontrol} \times 100 \quad (2)$$

2.5.9. The inhibitory effects of drug-loaded niosomes on HIV- 1 replication

The anti-Scr HIV activity was measured by using single-cycle replication assay. Briefly, single cycle replicable HIV virions (Scr HIV) were generated as Zabihollahi, Rezvan reported [57]. Then, HEK-293 T cells were seeded in a 6-well plate and transfected with three different plasmids (pSPAX2, pMD2G plasmids and pmzNL4-3) by using Turbofect transfection reagent (Fermentas). Viral supernatants were cultured for 24, 48 and 72 h after transfection procedure, then centrifuged at 10,000×*g* for 10 min, and filtered via 0.22 μm filters. Virions were stored at −70 °C and infectious titers were determined by the ELISA method [58]. To investigate the anti-Scr HIV effect of Tenofovir, PEG-NI, Empty PEG-NI, TAT-NI1 and Cys-TAT peptide, Hela cells were seeded and incubated into the 6-wells plate (5×10^5 cells per well, 18hr at 37 °C), and then, HIV virions were added to each well (600 ng P24/well) and incubated for 5hr at 37 °C. After the removal of extra free virions by fresh medium (DMEM medium with FBS 10%), 200 μl of infected HeLa cells were added to each well of the 96-well plate. Then, 100 μl of different treatments (0.15, 0.75, 1.25, 5 and 10 μM) were loaded to each well and incubated for 72 h at 37 °C. In order to investigate P24 load of supernatant (it is a structural protein of HIV and a significant marker of viral infection), a P24 capture ELISA kit (Biomerieux) was applied based on the ELISA kit's protocol. The UV absorbance was evaluated at 490 nm and the HIV inhibitory rate was measured by Eq. (3).

$$\frac{\text{AverageP24wasproductedbytreatment} - \text{AverageP24wasproductedbycontrol}}{\text{AverageP24wasproductedbycontrol}} \times 100 \quad (3)$$

2.5.10. Statistical analysis

Design-Expert version 8.0 was used for experimental design and its statistical analysis. All experiments were done in three independent experiments. For MTT assay, anti-Scr HIV efficacy and *in vitro* drug release, the graphs were plotted using Graph Pad Prism version 8.3.0. All data were reported as mean ± SD and were statistically analyzed using one-way analysis of variances (ANOVA) followed by the post-Tukey test. The p-value < 0.05 was considered as a significant difference.

3. Results

3.1. Characterization of functionalized DSPE-PEG2000-Maleimide

Thin-layer chromatography (TLC) was used for primary identification of reaction completion and DSPE-PEG2000-TAT formation (Fig. 2C-F). As shown in (Fig. 1B), the disappearance of the DSPE-PEG2000-Maleimide spot from the reaction mixture was confirmed by iodine vapor.

The H NMR and FTIR spectra of DSPE-PEG2000-Maleimiede and DSPE-PEG2000-TAT were shown in Fig. 1C-F. In the FTIR spectra of DSPE-PEG2000-MAL (Fig. 1C), a weak C═O stretch band at 1686.21 cm^{-1}, and an N—H stretch band at 3600–3200 cm^{-1} were found which may be responsible for the amide groups in DSPE-PEG2000-MAL. The intensity of the two bands in the spectrum of DSPE-PEG2000-TAT were remarkably enhanced (Fig. 1D), which should be due to the increased number of amide groups compared with DSPE-PEG-MAL. The results suggested that the TAT peptide had been conjugated to DSPE-PEG-MAL in the H NMR spectrum of DSPE-PEG2000-TAT (Fig. 1F). The Maleimide had a characteristic peak at 6.7 ppm (Fig. 1E). This peak disappeared in the H NMR spectrum of DSPE-PEG2000-TAT and two characteristic peaks at (5–5.5) ppm were observed (Fig. 1F). According to the results, it can be suggested that thiol group of Cys-TAT had completely reacted with the Maleimide group of lipids. As illustrated in Fig. 1E and F, the characteristic resonance peak of 7.400 ppm was the solvent residual peak and the characteristic peaks of PEG

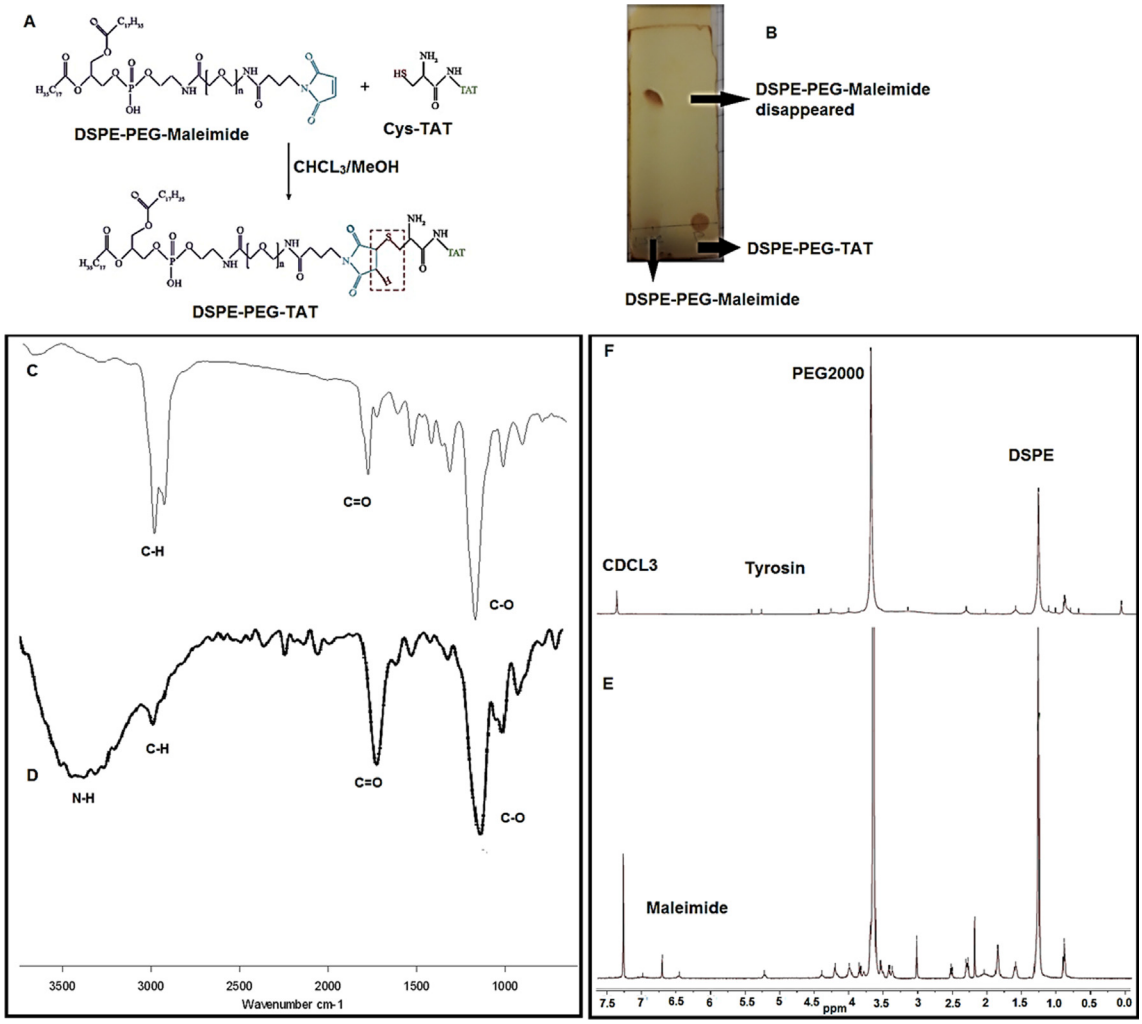

Fig. 1. DSPE-PEG2000-TAT Peptide characteristics; Schematic representation of TAT peptide conjugation to DSPE-PEG2000-MAL lipid (A) DSPE-PEG-TAT TLC (B) FTIR spectra of DSPE-PEG2000-MAL (C) FTIR spectra of DSPE-PEG2000-TAT (D) H NMR spectra of DSPE-PEG2000-MAL (E) H NMR spectra of DSPE-PEG2000-TAT (F).

(3.600 ppm) and the methylene protons peaks of DSPE (1.200 ppm) were shown too.

3.2. Formulation optimization

Response surface experimental design was used to indicate the effect of preparation variables on noisome characteristics as particle size, PDI and EE. The observed results are listed in Table 5. Accordingly, all of them had negative charges, the particle size of 150–231 nm, PDI about 0.3 and EE% of 55–89. Also, the niosomes loaded with Tenofovir exhibited similar particle sizes and narrow particle size distributions.

Response data of all formulations were fitted to the quadratic model as suggested via Design-Expert® software. Quadratic models correlating the relationship between the factors and responses were made and shown below:

$$Y_1 = 227.00 - 12.84\,X_1 - 18.57X_2 - 5.69\,X_1\,X_2 - 23.06\,X_1^2 - 52.16\,X_2^2$$

$$Y_2 = 0.27 - 0.023\,X_1 - 0.022\,X_2 + 0.016\,X_1\,X_2 + 0.037\,X_1^2 - 0.052\,X_2^2$$

$$Y_3 = 82.12 - 10.33\,X_1 - 1.67\,X_2 + 2.25\,X_1\,X_2 - 6.07\,X_1^2 - 16.07\,X_2^2$$

(Y_1 = mean size, Y_2 = PDI, Y_3 = EE, X_1 = molar ratio of lipid/drug and X_2 = molar ratio of Span 60/Cholesterol)

Accordingly, Y_1 and Y_2 were settled at minimum and Y_3 at maximum level, while X_1 and X_2 are within the obtained range. The statistical validity of models was determined by the ANOVA in the Design Expert ®software. The ANOVA results for three responses is presented in Table 6. The results are represented in Fig. 2 as response surfaces (3D) and contour plots too.

Response surface graph of Y_1 (Fig. 2A) shows that the particle size of niosome was reduced by increasing X_1 and X_2. In addition, the response surface graph of Y_2 (Fig. 2B) indicates that PDI of PEGylated niosomes (PEG-NIs) was enhanced by decreasing X_1 and X_2. In the Response surface graph of Y_3, an inverse relationship displays between dependent factors and encapsulation efficiency (Fig. 2C).

According to ANOVA results (Table 6), the determination coefficient (R^2) for mean size and EE models were larger than 0.8. It indicates that over 80% of the variation in the responses could be explained by the developed models. The ANOVA result for the PDI model was above 0.6. When The "p" value of the models is lower than 0.05, the model term are meaningful. So for Y_1 and Y_3 the model terms were significant but for Y_2 was insignificant. F-values of model responses for mean size, PDI and EE were 8.06, 2.16 and 10.29, respectively which demonstrated that the lack of fit of both models was not significant relative to the pure error.

The optimized formulation was achieved at X_1:10, X_2:0.9 with the corresponding desirability (D) value of 0.867. This factor level combination predicted the responses Y_1:217 nm, Y_2:0.335, Y_3:86% (Table 7). The optimized formulation (PEG-NI) was prepared three times for evaluation and indicating the success of the design.

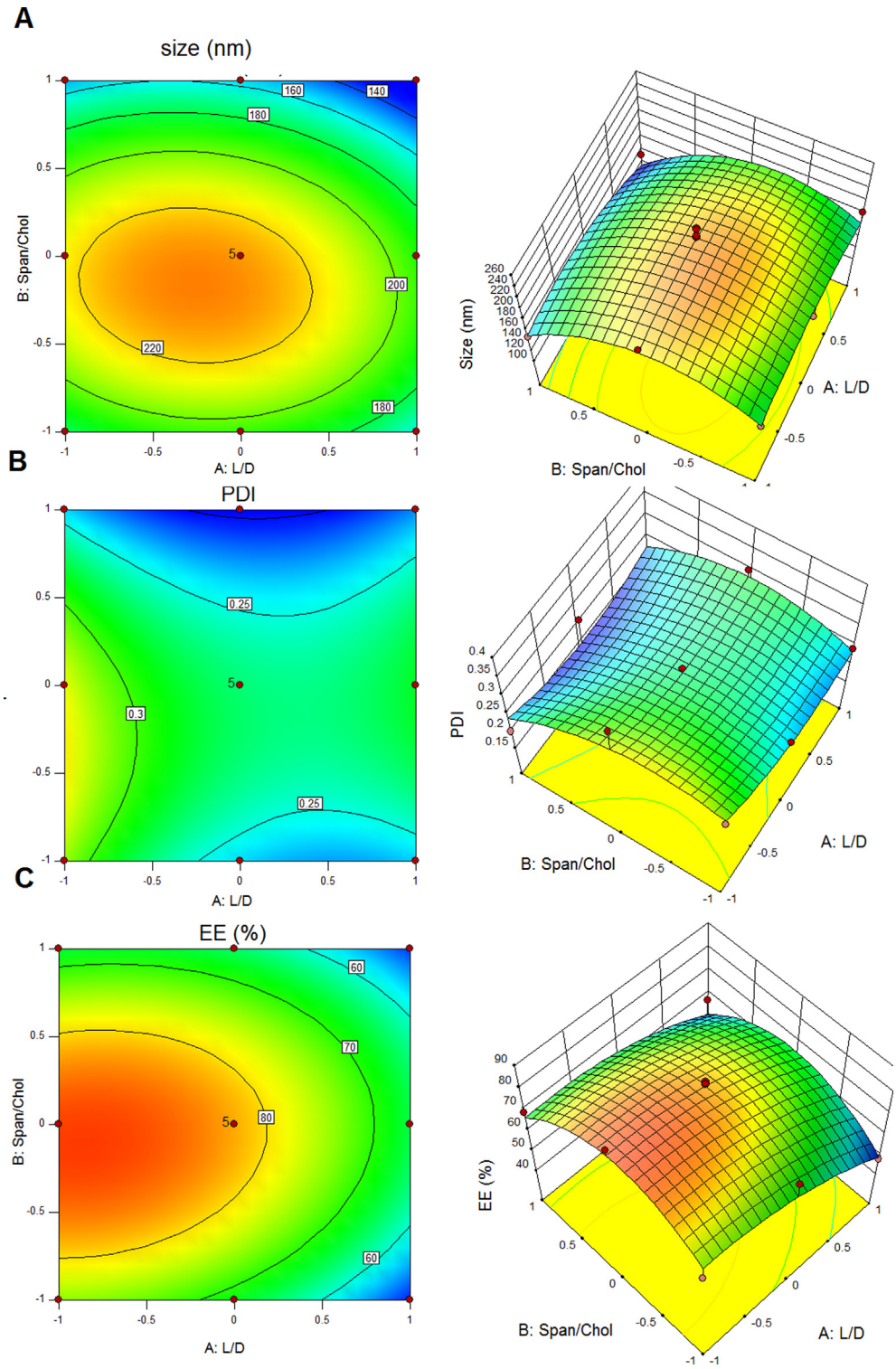

Fig. 2. Response surface and its Contour plot shows effect of X1 and X2 on vesicle size (A) Response surface and its Contour plot shows effect of X1 and X2 on PDI (B)) Response surface and its Contour plot shows effect of X1 and X2 on EE (C).

3.3. Characterization of optimum formulation

3.3.1. Physicochemical characterization

Table 8 is representing the physicochemical properties of different formulations of drug-loaded TAT conjugated niosomes including size, PDI and encapsulation efficacy. As shown, all samples had negative charges, mean size of 199–208 nm, PDI about 0.39 and EE above 70 percent. These TAT-NIs formulations exhibited almost similar mean sizes and narrow particle size distributions. The mean size of TAT-NI formations were slightly increased in comparison with PEG-NIs. After TAT conjugation on the surface of PEG-NI niosomes, the zeta potential has decreased from around −3 to −5.85 mv. This result would prolong the niosome circulation time.

Table 5
Observed RSM response for Tenofovir-loaded PEGylated niosome.

Sample ID	Mean size (μm)	PDI	EE (%)[1]
PEG-NI1	148.1	0.20	69
PEG-NI2	222	0.37	89
PEG-NI3	175.9	0.30	69
PEG-NI4	131.2	0.20	57
PEG-NI5	156	0.29	60
PEG-NI6	181.8	0.24	48
PEG-NI7	143.4	0.25	55
PEG-NI8	231.4	0.26	83
PEG-NI9	176.4	0.24	74

1: Encapsulation Efficiency percent.

Table 6
ANOVA result for four responses.

Response	*p*-value	R square(R^2)	F-value
Y_1(particle size)	0.01	0.85	8.06
Y_2(PDI)	0.17	0.60	2.16
Y_3(EE)	0.00	0.88	10.29

Table 7
The predicted and observed responses after RSM optimization.

Source	Mean size ± SD (nm)	PDI ± SD	EE(%) ± SD
predicted	217	0.33	86.00
observed	154.8 ± 2.6	0.262 ± 0.032	71.00 ± 0.01

Table 8
Physicochemical characterization of Tenofovir-loaded TAT conjugated niosomes.

Sample ID	Z-average size (nm)	PDI	Zeta potential(mv)	EE (%)
TAT-NI1	208.9	0.39	−5.85	75
TAT-NI2	217.4	0.40	−2.59	70
TAT-NI3	199.4	0.41	−3.47	72

The encapsulation efficiency percent of TAT-NI1 were better than TAT-NI2 and TAT-NI3 leading to its selection for further morphology investigations and cell study.

3.3.2. Morphology evaluation

Based on SEM image shown in Fig. 3, the obtained formulation of TAT-NI1 was possessed spherical shape with no visible aggregation. Also the niosome mean particle size was in the suitable range and similar to the size captured by DLS.

3.3.3. Cellular uptake

The HeLa cells were stained with fluorescent dye, Nile Red-loaded niosome with similar composition to confirm that the developed formulation could penetrate the cell membrane. As shown in Fig. 4C, D, the HeLa cells were well stained by the Nile Red-loaded niosomes and the niosomes located near the nuclei of the cells.

3.3.4. Drug-carrier interactions

The FT-IR spectra of the TAT conjugated niosomes indicated the successful formation of niosome (Fig. 5A-C). The N—H stretching vibration was shown in the region of 3470 cm^{-1} that is due to the functional group of TAT peptide. The strong characteristic band in the region 3414 cm^{-1} was due to the existence of the OH stretching vibration of the cholesterol and Span 60 molecules. The C═O stretching vibration was observed at 1640 cm^{-1} that was indicative of Span 60, DSPE-PEG-TAT and DSPE-PEG-PE. In addition, the intense band at 2920 cm^{-1} was assigned to the C—H stretching vibration of DSPE-PEG-TAT and DSPE-PEG-PE. The band in the region 1083 cm^{-1} was due to the C—O stretching vibration of DSPE-PEG-TAT, DSPE-PEG-PE, Span 60 and Tenofovir. The FTIR of Tenofovir-loaded TAT-NI1 showed a remarkable increase in the intensity of bands in 1083 cm^{-1} and 983 cm^{-1} which were due to phosphate ester stretching vibration of Tenofovir disoproxil fumarate [59].

Cholesterol showed an endothermic peak at 150 °C in DSC thermograms. Tenofovir and Span 60 thermograms showed a strong endotherm around 170 °C and 55 °C corresponding to their melting points. Fig. 5D shows DSC thermograms of empty and Tenofovir-loaded TAT-NI1. Accordingly, endothermic peaks of cholesterol, Span 60 and Tenofovir were disappeared and two similar peaks were shown around 37 °C belonging to empty and Tenofovir-loaded TAT-NI1 [60].

3.4. Release of Tenofovir from optimum niosomal formulations

Fig. 6A shows the release profile of Tenofovir from a dialysis bag containing TAT-NI1, PEG-NI and free Tenofovir samples. The results represented a similar and sustained release manner with an initial burst release (Fig. 6). TAT-NI1 formulation indicated slower cumulative drug release percent than PEG-NI under the same condition. The cumulative release percent of PEG-NI was 95% but for TAT-NI1 was 67.7% within 6 h. After 72 h PEG-NI could release 100% of Tenofovir while TAT-NI1 released 78% of the drug. Also, both of Tenofovir release profiles followed the sustained release in 2 phases, initially rapid release phase, and a subsequent slow release phase. Basically when the reservoir systems such as niosomes placed in the release environment, the drug which has diffused to the external membrane was released immediately

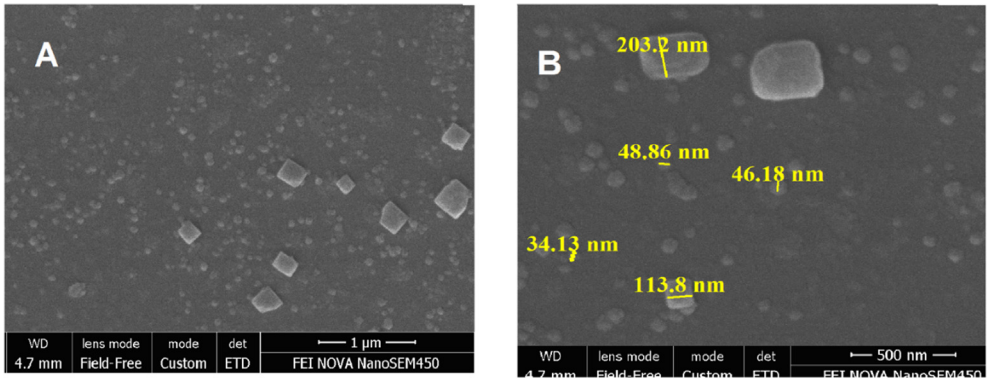

Fig. 3. Scanning electron microscopy of Tenofovir niosome (TAT-NI1) formulation.

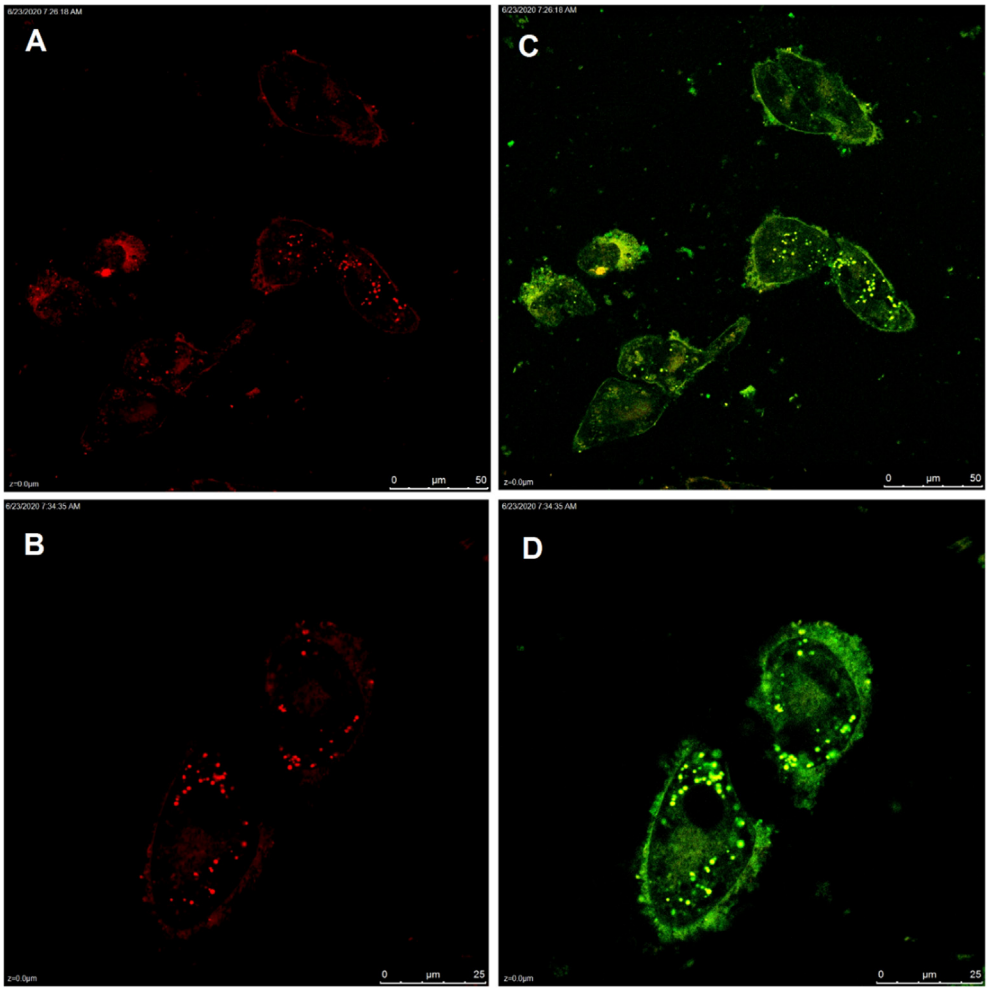

Fig. 4. Confocal images of HeLa cells incubated for 16 h with Nile Red-loaded TAT-NI1 (A-D). Nile Red-loaded TAT-NI1 staining (A, B), overlapped of Nile Red-loaded TAT-NI1 and plasma membrane staining (C, D). (For interpretation of the references to colour in this figure legend, the reader is referred to the web version of this article.) (For interpretation of the references to colour in this figure legend, the reader is referred to the web version of this article.)

and caused the burst release [61]. Also, the subsequent slow release phase occurred after bilayers degradation [62].

3.5. Physical stability study of Tenofovir-loaded niosomes

Breaking down or aggregation of niosomes during the storage process could change their shelf time. Therefore, the stability of TAT-NI1 during the storage was studied at two different temperatures (25 °C and 4 °C) and different time-interval by measuring the mean size, PDI and % EE of the TAT-NI1 sample. As shown in Fig. 7, there was a significant increase in mean size and PDI and decrease in EE of TAT-NI1 overtime at two different storage temperatures. These results indicated that developed niosomal formulation did not have physical stability.

3.6. In vitro cytotoxicity study

The cytotoxicity of the optimized Tenofovir-loaded PEGylated niosome (PEG-NI), Tenofovir-loaded TAT-NI1 (TAT-NI1), free drug, TAT peptide and empty PEG-NI were investigated by MTT assay on HeLa cell line after 48 h of incubation (Fig. 8). All of the treatments exhibited specified dose-dependent cytotoxicity on HeLa cells. TAT-NI1 showed higher cytotoxicity effect than PEG-NI. The IC_{50} values of treatments were represented in Table 9 and analyzed by Graph pad prism 8.3.0 software.

3.7. Evaluating the inhibitory effects of Tenofovir-loaded niosomes on HIV-1 replication

The anti-HIV1 efficacy of PEG-NI, TAT-NI1, empty PEG-NI, free drug and TAT peptide was evaluated at different non-toxic concentrations (150, 750, 1250, 5000 and 10^4 nM) after 72 h incubation on HIV infected HeLa cells in the presence of HIV virion. Anti-Scr HIV-1 effects of all treatments displayed a dose-dependent manner (Fig. 9). Employing both TAT-NI1 and PEG-NI showed stronger inhibitory effects than free Tenofovir at different doses. TAT-NI indicated weaker anti-HIV-1 effects than PEG-NI.

4. Discussion

Although extensive researches have been carried out on novel drug delivery systems to treat and diagnose of wide type of diseases, like HIV, there are limitations including toxicity and unsuitable immune responsibility in this field [63,64]. Several strategies have been suggested to overcome these drawbacks. For example, PEGylation of nano-based drug delivery systems can reduce the immunogenicity and enhance the half-life and flexibility of peptide bindings [38]. The surface targeting approach is another policy for improving therapeutic effects. For instance, conjugation of TAT peptide to various cargoes can increase physiological barrier penetration [39]. Therefore, the present study was designed to provide

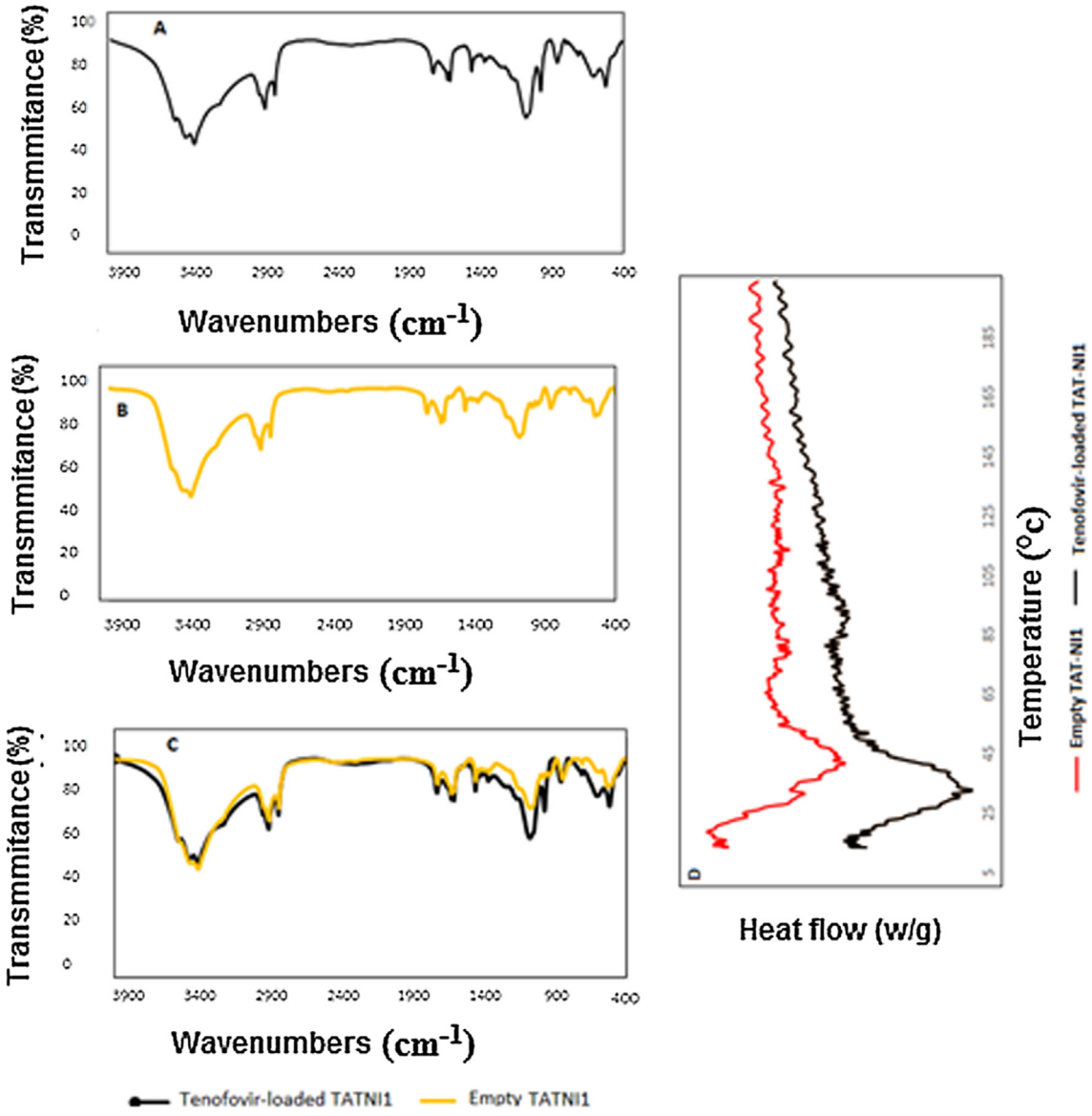

Fig. 5. FTIR of empty TAT-NI1 and TAT-NI1 (A-C), DSC thermograms of empty TAT-NI1 and TAT-NI1 (D). (Empty TAT-NI1: Empty TAT conjugated niosome, TAT-NI1: Tenofovir-loaded TAT conjugated niosome).

an effective Tenofovir drug delivery system based on TAT conjugation, against HIV-1 infection for the first time. To obtain optimum niosomal formulation, the influence of various preparation parameters must be considered. In this regard, response surface methodology was used to improved niosomal formulation with at least runs. According to earlier researches, particle size was considered as a major limiting parameter for the characterization of lipid nanocarriers, which remarkably affects stability, entrapment efficiency, bioavailability, bio-distribution, and drug penetration [65]. Entrapment efficiency is another limiting parameter for nanocarriers. Indeed, high Entrapment efficiency led to formatting (or shaping) niosomes with low total mass and the extensive amount of drug [66]. The entrapment of hydrophobic drugs such as Tenofovir in lipid bilayer affects the preparation process directly. Polydispersity index is another critical attribute that can indicate size distribution and homogeneity of the dispersions [67]. According to a much earlier published paper, cholesterol content had an important effect on niosomal particle size and EE% [68]. While cholesterol enrichment can increase EE by stabilizing the niosomal membrane and reducing the permeability of the lipid bilayer, the exceeding enhancement can disrupt the regularity of the lipid membrane, compete with the drug for packing within the bilayer and finally decrease the EE [69]. Also, Non-ionic, biodegradable and biocompatible surfactants like Spans can affect the EE and particle size of niosomes [70]. As well as, the interaction of cholesterol and surfactant in niosomal bilayer can increase the width of niosomal layer and thus enhance niosomal mean size afterward [71]. Furthermore, previous researches have shown that lipid/drug molar ratio can affect both particle size and EE [72]. However, by increasing drug concentration in the lipid bilayer, the encapsulation efficiency is improved but particle size grows up. Based on bilayer planar fragments (BPFs) theory, the lipid concentration enrichment in the niosomal formation can increase the number of Small Uni-lamellar Vesicles (SUVs), so it can enrich the thickness of the niosome and therefore it can elevate the mean size of niosomes [73]. Accordingly, the molar ratio of Span 60/cholesterol and lipid/drug was selected as an independent attribute in Tenofovir-loaded PEGylated niosome formulation optimization. Based on pointed literature reviews, the particle size, PDI and EE were selected as dependent features. According to

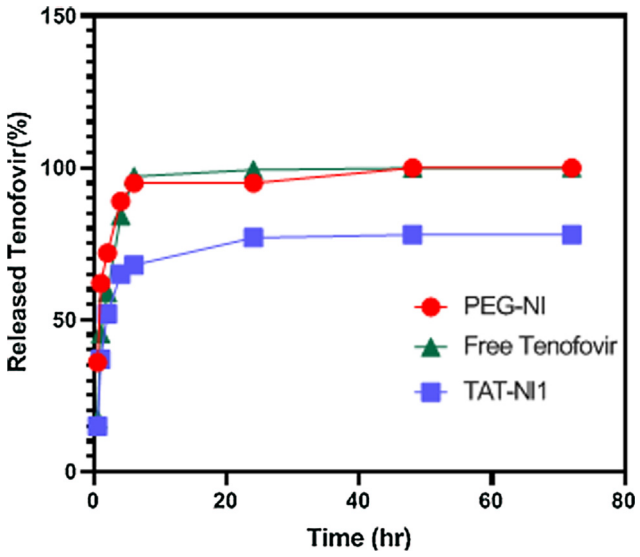

Fig. 6. Cumulative release profile of free Tenofovir and Tenofovir from Tenofovir loaded TAT-NI1 and PEG-NI.

our one-way ANOVA results, lipid/drug molar ratio enhancement led to niosomal mean size reduction, homogeneity improvement and encapsulation efficiency decrease. Therefore, by selecting the lipid/drug molar ratio at the lowest level, we will have bigger niosomes. In agreement with previous researches, cholesterol content can have two different effects on EE. Also, the interaction of Span and cholesterol has a critical impact on encapsulation efficiency. Based on our optimization results, the molar ratio of Span 60/cholesterol displayed an inverse relationship to Tenofovir encapsulation efficiency. Moreover by reducing this parameter, niosomal particle size will be increased which this outcome can prove previous reports. Span 60/cholesterol molar content has a positive effect on PDI, so increasing this molar ratio can improve the homogeneity of the niosomal system.

TAT peptide is a cell-penetrating peptide derived from HIV *trans*-activator of transcription protein. This cell-penetrating peptide typically has a positive charge which consists of a short stretch of basic amino acids (protein transduction domain) and can translocate peptide across the cellular membrane [74]. So, TAT peptide conjugation can improve the delivery of different types of therapeutics through the plasma membrane and enhance the efficacy of treatments afterward. These characteristics depend on several factors including the nature of targeted tissue. As reported previously, TAT modification of liposome can improve drug delivery in the brain and especially glioma tissues while it doesn't display any significant delivery enhancement in heart, spleen and liver tissue as compared to unconjugated liposome [67]. Actually, the route of administration has a critical impact on TAT conjugation efficiency. For example, because of faster kinetic removal of TAT conjugated delivery system in comparison with unconjugated, administration via intravenous rout was not an appropriate choice for TAT conjugated therapeutics [30]. Besides, the efficiency of drug delivery by TAT modification is dependent on the component of the nanocarrier. For instance, TAT modification of lipoplex containing DOTAP surfactant improves gene delivery in 30 M percent across Cos-7 cells, but reduces delivery efficiency in 50 mol percent [75]. Also, the PEGylation of liposomes, which is essential for long circulation time, reduced the uptake efficiency of TAT modified PEGylated liposome in special molar PEG ratio and PEG length. This principle lies in the steric effect of the PEG which hindered the interaction between the nanocarriers with the targeted cells [31]. Based on our study, conjugation of TAT peptide on optimized PEGylated niosome improved encapsulation efficiency and zeta potential, so this conjugation could lead to entrap more Tenofovir molar content by niosomes with higher shelf life. Increasing particle size and PDI were not considerable. The characteristic peaks of Tenofovir were disappeared in the TAT-NI1 sample thermogram. This disappearance proved previous reports and it was due to drug and niosomal components interaction and Tenofovir incorporation within the niosomal bilayer [42]. Briefly, TAT-NI1 morphological studies displayed spherical and homogenous particles without any aggregation. Also, the DLS method showed a larger mean particle size while SEM showed a smaller one. This achievement might be due to the drying process during SEM imaging. In other words, SEM represented the mean size of dried nanoparticles (measures the exact diameter of each particle). However, DLS measured the hydrodynamic diameter that included core plus any molecule attached or adsorbed on the surface, including ions and water molecule [67].

In vitro cytotoxicity studies showed higher IC50 for PEG-NI than free Tenofovir on the HeLa cell line. This can be due to the reduction in the diffusive uptake process of PEGylated niosome compared to free Tenofovir [42]. Besides, our MTT assay indicated that the toxic effect of all treatments on the HeLa cell line was dose-dependent manner. Also, Tenofovir-loaded TAT conjugated niosome (TAT-N1I) displayed a higher cytotoxic effect than TAT-unconjugated niosome (PEG-NI) and free drug. This achievement confirmed the previous researches that indicated toxic nature of TAT peptide and conjugation of this CPP to cargoes showed a higher toxic effect than unconjugated forms as explained by the high affinity of TAT peptide to HeLa cell line, too [76].

Anti-Scr HIV1 investigation of all treatments represented a dose-dependent manner on the HIV infected HeLa cells. Also, TAT conjugated (TAT-NI1) and un-conjugated (PEG-NI) niosomal formulation could significantly increase the inhibitory effect of free Tenofovir against HIV1 virion. Our results illustrated that the

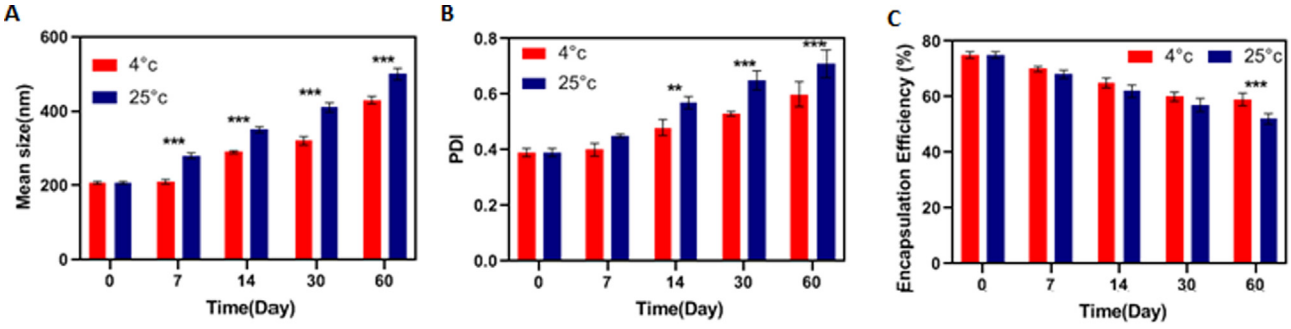

Fig. 7. the effect of storage at different temperatures on mean size (A), PDI (B), and Tenofovir encapsulation efficiency (EE) (C) of the TAT-NI1 sample. Data are represented as Mean ± SD, n = 3, (** *p*-value < 0.01 and *** *p*-value < 0.001).

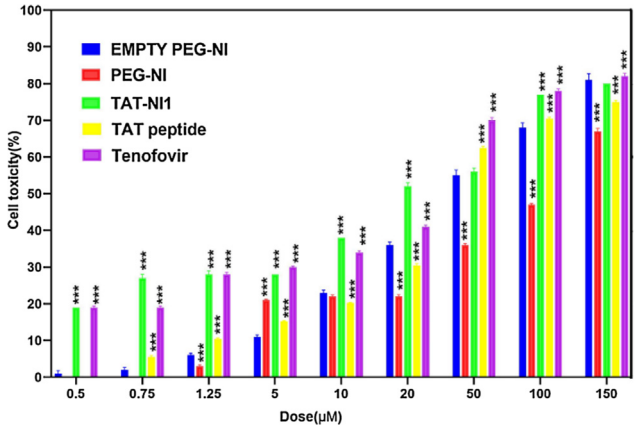

Fig. 8. The cytotoxicity activity of treatments in different doses on HeLa cells after 48hr. The error-bars represent the standard deviation from the mean (N = 3, *** p-value < 0.001). (Empty PEG-NI: Empty PEGylated niosome, PEG-NI: Tenofovir-loaded PEGylated niosome, TAT-NI1: Tenofovir-loaded TAT conjugated niosome.)

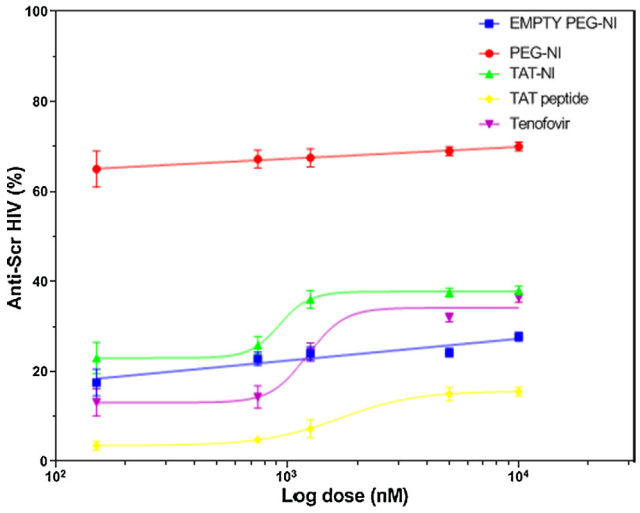

Fig. 9. Anti HIV-1 Efficacy of treatments in different doses on infected HeLa cell after 72hr incubation. The error-bars represent the standard deviation from the mean (N = 3). (Empty PEG-NI: Empty PEGylated niosome, PEG-NI: Tenofovir-loaded PEGylated niosome, TAT-NI1: Tenofovir-loaded TAT conjugated niosome).

Table 9
The IC50 values were calculated using Graph Pad Prism 8.3.0.

	PEG-NI	Empty PEG-NI	Tenofovir	TAT-NI1	TAT peptide
$IC_{50}(\mu M)$	65.41	37.04	43.07	41.02	37.12
R^2	0.922	0.995	0.978	0.968	0.983

enhancement of free TAT peptide could decrease the inhibitory effect of TAT-NI1 in comparison with PEG-NI on HIV infected HeLa cells. This achievement might be explained by the existence of the transduction domain of TAT peptide which could support Scr HIV virion entrance. Therefore, this outcome caused a lower inhibitory effect for Tenofovir-loaded TAT conjugated niosome rather than un-conjugated forms. According to the pointed literature reviews, the TAT conjugation efficiency also might be due to the surfactant content of PEG molar ratio. The release profile of Tenofovir might be another reason for low potency of inhibition. According to the result of release profile, TAT peptide conjugation on the surface of nanocarrier led to slower cumulative drug release of TAT-NI1 through 72hr in contrast with PEG-NI. It may be reclined in TAT hydrophilic nature that decorates the surface of niosomal formulation which was loaded with hydrophobic Tenofovir anti HIV drug (TAT-NI1). Based on the previous studies, TAT conjugation can enhance nanocarrier internalization through the endocytosis pathway into Hela cells [77]. On this basis, confocal electron microscopy showed successful uptake for Tenofovir-loaded TAT conjugated noisome into Hela cells.

5. Conclusion

To date, several studies have proved the benefit of TAT peptide conjugation in nano-based drug delivery systems. However, the obtained results in the current study indicated that TAT peptide conjugated niosome had a lower anti-viral effect than PEGylated samples. We concluded that the anti-HIV effects of Tenofovir-loaded niosomes on infected HeLa cells have been enhanced through PEGylation and TAT peptide conjugation. Furthermore, TAT peptide niosomal surface decoration could improve the drug release profile. The current study revealed that this conjugation could improve Tenofovir encapsulation efficiency and niosomal shelf life. So, PEGylated niosomal formulation is preferred against TAT peptide conjugation in anti-HIV cases.

Funding

This research was financially supported by Grant 1048 Pasteur Institute of Iran.

Declaration of Competing Interest

The authors declare that they have no known competing financial interests or personal relationships that could have appeared to influence the work reported in this paper.

Acknowledgments

The authors would like to acknowledge the Pasteur Institute of Iran for providing the necessary laboratory facilities for this study.

Ethics approval and consent to participate

There are no “human subjects” in this study.

Appendix A. Supplementary data

Supplementary data to this article can be found online at https://doi.org/10.1016/j.apt.2021.05.047.

References

[1] Y.-H. Zheng, N. Lovsin, B. Peterlin, Newly identified host factors modulate HIV replication, Immunol. Lett. 97 (2005) 225–234.
[2] B. Nuyen, J. Glick, V. Ferrel, HIV/AIDS, Equal Curric. (2019) 199–221.
[3] Global hiv statistics 2020[Fact sheet].
[4] S.H. Notaro, HIV/AIDS, Marginality and Global LGBT Communities, Conflicts, civil rights and controversy, Palgrave Macmillan, 2020, pp. 75–110.
[5] V.B. Oti, Nanoparticles and Its Implications in HIV/AIDS Therapy, Curr. Drug Discov. Technol. 17 (2020) 448–456.
[6] J.R. Azanza, E.G. Quetglas, B. Sadaba, A. Gomez-Giu, Tenofovir: pharmacology and interactions, Enfermedades Infecciosasy Microbiologia Clinica 26 (2008) 2–6.
[7] K. Matlhola, K.-S. Lebogang, Formulation and Optimization of Eudragit RS PO-Tenofovir Nanocarriers Using Box-Behnken Experimental Design, J. Nanomater. (2015) 1–11.
[8] K. Tahara, Pharmaceutical formulation and manufacturing using particle/powder technology for personalized medicines, Adv. Powder Technol. 31 (2020) 387–392.

[9] J.K. Patra, G. Das, L.F. Fraceto, et al., Nano based drug delivery systems: recent developments and future prospects, Nanobiotechnol 16 (2018) 1–33.
[10] P. Vishal, V. Sanklecha, Review on Niosomes, Austin Pharmacol. Pharm. 3 (2018).
[11] F. Haghiralsadat, G.H. Amoabediny, S. Naderinezhad, et al., Overview of Preparation Methods of Polymeric and Lipid-Based (Niosome, Solid Lipid, Liposome) Nanoparticles: A Comprehensive Review, Int. J. Poly. Mater. Poly. Biomater. 67 (2017) 383–400.
[12] D. Ag Seleci, M.J.-G. Walter, F. Stahl, Niosomes as Nanoparticular Drug Carriers: Fundamentals and Recent Application, J. Nanomater. (2016).
[13] D. Lombardo, M.A. Kiselev, M.T. Caccamo, Smart Nanoparticles for Drug Delivery Application: Development of Versatile Nanocarrier Platforms in Biotechnology and Nanomedicine, J. Nanomater. (2019).
[14] K. Tahara, H. Tomida, Y. Ito, S. Tachikawa, R. Onodera, H. Tanaka, Y. Tozuka, H. Takeuchi, Pulmonary liposomal formulations encapsulated procaterol hydrochloride by a remote loading method achieve sustained release and extended pharmacological effects, Int. J. Pharm. 505 (2016) 139–146.
[15] G.D. Venkatasubbu, S. Ramasamy, V. Ramakrishnan, J. Kumar, Folate targeted PEGylated titanium dioxide nanoparticles as a nanocarrier for targeted paclitaxel drug delivery, Adv. Powder Technol. 24 (2013) 947–954.
[16] K. Tahara, Y. Kato, H. Yamamoto, J. Kreuter, Y. Kawashima, Intracellular drug delivery using polysorbate 80-modified poly(D, L-lactide-co-glycolide) nanospheres to glioblastoma cells, J. Microencapsul. 28 (2011) 29–36.
[17] H. Fu, S.H. Kairong, G. Hu, Y. Yang, et al., Tumor-Targeted Paclitaxel Delivery and Enhanced Penetration Using TAT-Decorated Liposomes Comprising Redox-Responsive Poly(Ethylene Glycol), J. Pharm. Sci. 104 (2014) 1160–1173.
[18] M. Jafari, A. Rezvanpour, Upconversion nano-particles from synthesis to cancer treatment: A review, Adv. Powder Technol. 30 (2019) 1731–1753.
[19] L. Kong, F. Campbell, A. Kros, DePEGylation strategies to increase cancer nanomedicine efficacy, Nanoscale Horiz. 4 (2019) 378–387.
[20] R. Wang, R. Xiao, Z.H. Zeng, L. Xu, J. Wang, Application of poly(ethylene glycol)–distearoylphosphatidylethanolamine (PEG-DSPE) block copolymers and their derivatives as nanomaterials in drug delivery, Int. J. 7 (2012) 4185–4198.
[21] P. Marqués-Gallego, A. Kroon, Ligation Strategies for Targeting Liposomal Nanocarriers, Biomed Res. Int. (2014).
[22] E. Paszako, M. Senge, Immunoliposomes, Curr. Med. Chem. 31 (2012) 5239–5277.
[23] Y. Liu, R. Ran, J. Chen, Q. Kuang, J. Tang, et al., Paclitaxel loaded liposomes decorated with a multifunctionalpeptide for glioma targeting, Biomaterials 35 (2014) 4835–4847.
[24] C.C. Berry, Intracellular delivery of nanoparticles via the HIV-1 tat peptide, Nanomedicine (2008) 357–365.
[25] S. Shan, S.H. Jia, T. Lawson, et al., The Use of TAT Peptide-Functionalized Graphene as a Highly Nuclear-Targeting Carrier System for Suppression of Choroidal Melanoma, Int. J. Mol. Sci. 20 (2019) 4454.
[26] A. Fittipaldi, M. Giacca, Transcellular protein transduction using the Tat protein of HIV-1, Adv. Drug Deliv. Rev. 57 (2005) 597–608.
[27] T. Zong, L. Mei, H. Gao, S.H. Kairong, J. Chen, et al., Enhanced Glioma Targeting and Penetration by Dual-Targeting Liposome Co-modified with T7 and TAT, J. Pharm. Sci. 103 (2014) 3891–3901.
[28] R.K. Deshmukh, J.B. Naik, The impact of preparation parameters on sustained release aceclofenac microspheres: A design of experiments, Adv. Powder Technol. 26 (2015) 244–252.
[29] J. Gil-Chávez, S.S.P. Padhi, U. Hartge, S. Heinrich, I. Smirnova, Optimization of the spray-drying process for developing aquasolv lignin particles using response surface methodology, Adv. Powder Technol. 31 (2020) 2348–2356.
[30] K. Kadota, T.R. Sosnowski, S. Tobita, I. Tachibana, J.E. Tse, H. Uchiyama, Y. Tozuka, A particle technology approach toward designing dry-powder inhaler formulations for personalized medicine in respiratory diseases, Adv. Powder Technol. 31 (2020) 219–226.
[31] G. Perfetti, D.E.C. van der Meer, W.J. Wildeboer, G.M.H. Meester, Investigation on resistance to attrition of coated particles by response surface methodology, Adv. Powder Technol. 23 (2012) 64–70.
[32] M. Hatami, Nanoparticles migration around the heated cylinder during the RSM optimization of a wavy-wall enclosure, Adv. Powder Technol. 28 (2017) 890–899.
[33] C.B. Garcia, D. Shi, T.J. Webster, Tat-functionalized liposomes for the treatment of meningitis: An in vitro study, Int. J. Nanomed. 12 (2017) 3009–3021.
[34] M. Teymouri, A. Badiee, S.H. Golmohammadzadeh, K. Sadri, et al., Tat peptide and Hexadecylphosphocholine introduction into Pegylated liposomal doxorubicin: an in vitro and in vivo study on drug cellular delivery, release, biodistribution and antitumor activity, Int. J. Pharm. 511 (2016) 236–244.
[35] R. Ran, H. Wang, Y. Liu, er al, Microfluidic self-assembly of a combinatorial library of single- and dual-ligand liposomes for in vitro and in vivo tumor targeting, Eur. J. Pharm. Biopharm. 130 (2018) 1–10.
[36] T. Zong, L. Mei, H. Goa, et al., Enhanced Glioma Targeting and Penetration by Dual-Targeting Liposome Co-modified with T7 and TAT, J. Pharm. Sci. 103 (2014) 3891–3901.
[37] H. Fu, S.H. Kairong, H. Guanlian, Y. Yuting, et al., Tumor-Targeted Paclitaxel Delivery and Enhanced Penetration Using TAT-Decorated Liposomes Comprising Redox-Responsive Poly(Ethylene Glycol), J. Pharm. Sci. 104 (2015) 1160–1173.
[38] J. Loureiro, B. Gomes, G. Fricket, et al., Dual ligand immunoliposomes for drug delivery to the brain, Colloids Surf. B, Biointerf. 134 (2015) 213–219.
[39] M. Li, S.H. Kairong, et al., pH-sensitive folic acid and dNP2 peptide dual-modified liposome for enhanced targeted chemotherapy of glioma, Eur. J. Pharm. Sci. 124 (2018) 240–248.
[40] L. Mei, L. Fu, K. Shi, Q. Zhang, Y. Liu, J. Tang, H. Gao, Z.H. Zhang, Q. He, Increased tumor targeted delivery using a multistage liposome system functionalized with RGD, TAT and cleavable PEG, Int. J. Pharm. 468 (2014) 26–38.
[41] D.A. Seleci, M. Seleci, F. Stahl, T.H. Scheper, Tumor homing and penetrating peptide conjugated niosomes as multi-drug carriers for tumor-targeted drug delivery, RSC Adv. 7 (2017) 33378–33384.
[42] S.H. Khoshtinat Nikkhoia, F. Rahbarizadeh, D. Ahmadvand, S.M. Moghimi, Multivalent targeting and killing of HER2 overexpressing breast carcinoma cells with methotrexate-encapsulated tetra-specific non-overlapping variable domain heavy chain anti-HER2 antibody-PEG-liposomes: In vitro proof-of-concept, Eur. J. Pharm. Sci. 122 (2018) 42–50.
[43] H. Wang, X. Wang, C. Xie, M. Zhang, H. Ruan, S. Wang, K. Jiang, F. Wang, C.H. Zhan, W. Lu, H. Wang, Nanodisk-based glioma-targeted drug delivery enabled by a stable glycopeptide, J. Control. Release 284 (2018) 26–38.
[44] I. Akbarzadeh, M. Fatemizadeh, F. Heidari, N. Mousavi Niri, Niosomal Formulation for Co-Administration of Hydrophobic Anticancer Drugs into MCF-7 Cancer Cells, Arch. Adv. Biosci. 11 (2020) 1–9.
[45] T. Dai, K. Jiang, W. Lu, Liposomes and lipid disks traverse the BBB and BBTB as intact forms as revealed by two-step Förster resonance energy transfer imaging, Acta Pharm. Sin. B 8 (2018) 261–271.
[46] Z. Belhadj, M. Ying, X. Cao, X. Hu, C.H. Zhan, X. Wei, J. Gao, X. Wang, Z.H. Yan, W. Lu, Design of Y-shaped targeting material for liposome-based multifunctional glioblastoma-targeted drug delivery, J. Control. Release 255 (2017) 132–141.
[47] I. Akbarzadeh, M. Tavakkoli Yaraki, S. Ahmadi, M. Chiani, D. Nourouzian, Folic acid-functionalized niosomal nanoparticles for selective dual-drug delivery into breast cancer cells: An in-vitro investigation, Adv. Powder Technol. 31 (2020) 4064–4071.
[48] W. Yang, Q. Hu, Y. Xu, H. Liu, L. Zhong, Antibody Fragment-conjugated Gemcitabine and Paclitaxel-based liposome for Effective Therapeutic Efficacy in Pancreatic Cancer, Mater. Sci. Eng. C 89 (2018) 328–335.
[49] S.H. Hashemi, M. Montazer, N. Naghdi, T. Toliyat, Formulation and characterization of alprazolam-loaded nanoliposomes: screening of process variables and optimizing characteristics using RSM, Drug Dev. Ind. Pharm. 44 (2018) 296–305.
[50] H. Gogoi, R. Mani, R. Bhatnagar, A niosome formulation modulates the Th1/Th2 bias immune response in mice and also provides protection against anthrax spore challenge, Int. J. Nanomed. 13 (2018) 7427–7440.
[51] F. Heidari, I. Akbarzade, D. Nourouzian, A. Mirzaee, H. Bakhshande, Optimization and characterization of tannic acid loaded niosomes for enhanced antibacterial and anti-biofilm activities, Adv. Powder Technol. 31 (2020) 4768–4781.
[52] S. Mandal, Y. Zhou, A. Shibata, C.H. Destache, Confocal fluorescence microscopy: An ultra-sensitive tool used to evaluate intracellular antiretroviral nano-drug delivery in HeLa cells, AIP Adv. 8 (2015) 084803.
[53] D. Seleci, M. Seleci, A. Jochums, J. Walter, F. Stahl, T. Scheper, Aptamer mediated niosomal drug delivery, RSC Adv. 6 (2016) 87910–87918.
[54] N. Ohnishi, S. Tanaka, K. Tahara, H. Takeuchi, Characterization of insulin-loaded liposome using column-switching HPLC, Int. J. Pharm. 479 (2015) 302–305.
[55] K. Matlhola, L. Katata-Seru, l. Tshweu, et al., Formulation and Optimization of Eudragit RS PO-Tenofovir Nanocarriers Using Box-Behnken Experimental Design, J. Nanomater. (2015).
[56] S. Soleymani, F. Yari, A. Bolhassani, H. Bakhshande, Platelet microparticles: An effective delivery system for anti-viral drugs, J. Drug Delivery Sci. Technol. 51 (2019) 290–296.
[57] R. Zabihollahi, M. Sadat, R. Vahabpour, et al., Development of single-cycle replicable human immunodeficiency virus 1 mutants, Acta Virol. 55 (2011) 15–22.
[58] S. Soleymani, R. Zabihollahi, S. Shahbazi, A. Bolhassani, Antiviral Effects of Saffron and its Major Ingredients, Curr. Drug Deliv. 15 (2018) 698–704.
[59] R. Ghafelehbashi, I. Akbarzadeh, M. Tavakkoli Yaraki, A. Lajevardi, M. Fatemizadeh, L. Heidarpoor Saremi, Preparation, physicochemical properties, in vitro evaluation and release behavior of cephalexin-loaded niosomes, Int. J. Pharm. 569 (2018).
[60] Z. Sadeghi-Ghadi, R. Dinarvand, N. Asemi, et al., Preparation, characterization and in vivo evaluation of novel hyaluronan containing niosomes tailored by Box-Behnken design to to co-encapsulate curcumin and quercetin, Eur. J. Pharm. Sci. 130 (2019) 234–246.
[61] X. Huang, C.H. Brazel, On the importance and mechanisms of burst release in matrix-controlled drug delivery systems, J. Control. Release 73 (2001) 121–136.
[62] A. Sodagar Taleghani, P. Ebrahimnejad, A. Heydarinasab, A. Akbarzadeh, Sugar-conjugated dendritic mesoporous silica nanoparticles as pH-responsive nanocarriers for tumor targeting and controlled release of deferasirox, Mater. Sci. Eng. 98 (2019) 358–368.
[63] S. Soleymani, F. Yari, A. Bolhassani, An effective delivery system for anti-viral drugs, J. Drug Delivery Sci. Technol. 51 (2019) 290–296.
[64] K. Tahara, M. Kobayashi, S. Yoshida, R. Onodera, N. Inoue, Effects of cationic liposomes with stearylamine against virus infection, Int. J. Pharm. 543 (2018) 311–317.
[65] R.M.F. Sammour, M. Taher, B. Chatterjee, A. Shahiwala, S. Mahmood, Optimization of Aceclofenac Proniosomes by Using Different Carriers, Part 1: Development and Characterization, Pharmaceutics 11 (2019) 350.

[66] Z. Bayindir, N. Yksel, Investigation of Formulation Variables and Excipient Interaction on the Production of Niosomes, AAPS PharmSciTech 13 (2012) 826–835.
[67] P. Ebrahimnejad, Z. Sadeghi-Ghadi, Curcumin entrapped hyaluronan containing niosome: Preparation, characterization and in vitro/in vivo evaluation, J. Microencapsul. 36 (2019) 169–179.
[68] M. Kassem, H. El-Sawy, F. Abdallah, T. Abdelghany, K.H. El-Say, Maximizing the Therapeutic Efficacy of Imatinib Mesylate-Loaded Niosomes on Human Colon Adenocarcinoma Using Box-Behnken Design, J. Pharm. Sci. 106 (2017) 111–122.
[69] D. Fathalla et al., In-vitro and In-vivo Evaluation of Niosomal Gel Containing Aceclofenac for Sustained Drug Delivery, Int. J. Pharm. Sci. Res. 1 (2014) 1.
[70] M. Arafa, B. Ayoub, DOE Optimization of Nano-based Carrier of Pregabalin as Hydrogel: New Therapeutic & Chemometric Approaches for Controlled Drug Delivery Systems, Sci. Rep. 7 (2017) 1–15.
[71] S. Moghassemi, A. Hadjizadeh, Nano-niosomes as Nanoscale Drug Delivery Systems: An Illustrated Review, J. Controlled Release, Official J. Controlled Release Soc. 185 (2014) 22–36.
[72] G. Sailor, A.K. Seth, G. Parmar, S. Chauhan, A. Javia, Formulation and in vitro evaluation of berberine containing liposome optimized by 3 2 full factorial designs, J. Appl. Pharm. Sci. 5 (2015) 23–28.
[73] A.D. Sezer, J. Akbuga, A.L. Baş, In Vitro Evaluation of Enrofloxacin-Loaded MLV Liposomes, Drug Delivery 14 (2007) 47–53.
[74] E. Vivès, P. Brodin, B. Lebleu, A Truncated HIV-1 Tat Protein Basic Domain Rapidly Translocates through the Plasma Membrane and Accumulates in the Cell Nucleus, J. Biol. Chem. 272 (1997) 16010–16017.
[75] R. Vandenbroucke, S. De Smedt, J. Demeester, N. Sanders, Cellular entry pathway and gene transfer capacity of TAT-modified lipoplexes, BBA 1768 (2007) 571–579.
[76] M. Rizzuti, M. Nizzardo, C.H. Zanetta, A. Ramirez, S. Corti, Therapeutic applications of the cell-penetrating HIV-1 Tat peptide, Drug Discovery Today 20 (2015) 76–85.
[77] Y. Bi, R. Lee, X. Wang, Y. Sun, M. Wang, L. Li, C.H. Li, J. Xie, L. Teng, Liposomal codelivery of an SN38 prodrug and a survivin siRNA for tumor therapy, Int. J. Nanomed. 13 (2018) 5811–5822.